Air Qual Atmos Health
DOI 10.1007/s11869-014-0300-9

Elevated stacks' pollutants' dispersion and its contributions to photochemical smog formation in a heavily industrialized area

Lakhdar Aidaoui · Athanasios G. Triantafyllou · Abbes Azzi · Stylianos. K. Garas · Vasileios. N. Matthaios

Received: 15 August 2014 / Accepted: 30 September 2014

Abstract In this study, the photochemical smog formation over a heavily industrialized area with complex terrain was investigated. A mesoscale prognostic meteorological and air pollution model was used in combination with data, which were collected by in situ and remote monitoring stations. The area of interest is a mountainous basin in north-western Greece. The intensive industrial activity in this area has resulted in effects on the air quality of the area, mainly caused by the lignite-fired power stations and the lignite mining operation. The study focused on the dispersion of ozone production due to primary pollutants' emissions from the power stations (PSs). Moreover, the investigation of this external sources' contribution to the ozone concentrations measured in Kozani, the most populated city of the area, is ventured. The results showed a considerable skill of the model in predicting the major mesoscale features affecting the pollutants' dispersion and concentrations in the area of interest. Numerical simulation data of photochemical pollutants were significantly correlated with meteorology during the simulation period. The correlation reveals the most important factors of ozone production, such as solar radiation, temperature, wind speed and topography. The obtained results have contributed to the verification of distant pollutants' transfer from industrial sources.

Keywords Photochemical simulation · Meteorology effect · Industrial emissions · Mesoscale model · Ozone

L. Aidaoui (✉) · A. Azzi
Laboratoire Aero-Hydrodynamique Navale, Faculté de Génie Mécanique, Université des Sciences et de la Technologie d'Oran (USTO), Oran, Algeria
e-mail: laidaoui@gmail.com

A. G. Triantafyllou · S. K. Garas · V. N. Matthaios
Laboratory of Atmospheric Pollution and Environmental Physics, Technological Education Institute (TEI) of Western Macedonia, Koila, 501 00 Kozani, Greece
URL: http://airlab.teikoz.gr

Introduction

Atmospheric pollution grew with the increase of industrialization and became one of the most important environmental and public health concerns. Pollutants directly emitted from sources (primary pollutants) including NO_x, SO_2 and volatile organic compounds (VOCs), or formed in the atmosphere as the result of chemical transformation (secondary pollutants) e.g. ozone, are harmful to human health (Vlachokostas et al. 2010a). The combination of chemical substances and specific meteorological parameters is the cause for the formation of the ground-level ozone layer. The formation and accumulation of ozone at the ground level are dangerous for people with respiratory disorders (Bernard et al. 2001). Moreover, crop damages from photochemical air pollution constitute one of the most serious problems in the European agricultural sector at the present time (Vlachokostas et al. 2010b). Ozone has also a negative impact on forests, materials and ecosystems (Wang et al. 2005; Brunelli et al. 2007; Pontiggia et al. 2009; Linkov et al. 2009). High temperature, sunlight and increased surface pressure have been proven to cause ozone formation (Chen et al. 2003). In addition, local circulations e.g. see breeze (Moussiopoulos et al. 2006) may assist in ozone formation by creating adequate dilution conditions that accelerate photochemical reactions. Wind speed and direction have also been considered as important factors in the formation of ozone (Brulfert et al. 2005).

Current predictive capabilities must be improved to enable policymakers to reach balanced decisions on emission reduction strategies. This requires a thorough understanding of the processes and factors affecting the formation of pollutants and their concentrations. Such goal may be achieved through

Published online: 08 October 2014

monitoring networks, describing the spatial and temporal pollutants' distribution which is a crucial factor to evaluate the impact of photochemical pollution. (Palaciosa et al. 2002; Nam et al. 2006; Ling et al. 2011).

Air quality assessment for photochemical pollution makes use of air quality models to give information concerning the spatial and temporal distribution, as well as to predict how future concentrations will respond to emissions' controls. Given the complexity of the combined physicochemical phenomenon leading to ozone and other pollutants' formation, air quality models represent the best theoretical approach currently available to understand the response of the atmosphere and especially of the ozone levels to different air pollution control measures (Hurley et al. 2005; Dias de Freitas et al. 2005; Moussiopoulos et al. 2006; Di Sabatino et al. 2007; Yen-Ping Peng et al. 2011). However, if their ability to reproduce and describe historical photochemical pollution episodes has been demonstrated, the robustness of the predicted air quality resulting from emission changes still has to be proven (Gilliliand et al. 2008; Godowitch et al. 2011; Napelenok et al. 2011; Zhou et al. 2013). Photochemical air quality models take data on meteorology and emissions, couple the data with descriptions of the physical and chemical processes that occur in the atmosphere and numerically process the information to yield predictions of air pollutant concentrations as a function of time and location (Allen and Durrenberger 2002; Couach et al. 2003).

In this work, an attempt is made in order to investigate the photochemical smog formation and the prevailing flow pattern over a heavily industrialized mountainous basin in NW Greece. Six lignite-fired power stations are operated in the greater area resulting in large amount of PM, NO_x and SO_2 emissions in the atmosphere (Kaldellis et al. 2012; Triantafyllou et al. 2002). The study focuses on the dispersion of ozone produced by primary pollutants' emissions from PSs and on the contribution of these external sources to the O_3 concentrations measured in the most populated city of the area, Kozani. The city is located in a distance of about 12 km southerly to the most neighbouring PS. It is a complicated case in terms of source variety (i.e. coal-fired power plants' operation, mining activities, urban sources), ground complexity and prevailing meteorological conditions (Triantafyllou et al. 1995). The north basin of the city is governed by nocturnal stagnant conditions favouring ozone production and accumulation within the surface boundary layer during sunny days. Stack emissions may affect the city under specific meteorological conditions, which in combination with urban sources may cause air pollution episodes (Triantafyllou 2001; Triantafyllou et al. 2002).

A coupled mesoscale prognostic meteorological and air pollution model is used, in combination with data, which were collected by a conventional ground monitoring station (MS) and a differential optical absorption spectroscopy (DOAS) system. A seven-day period in the summer of 2006 was selected for simulation and, in particular, the 23–29 of June 2006. This period of the year was recorded as a period with high temperatures and elevated air pollutant concentrations in the city of Kozani. For the same period, experimental data from the MS and DOAS system have also been collected. The analysis of pollutants' concentrations and meteorological parameters reveals the most important factors of ozone production, such as solar radiation, temperature, wind speed and topography. The methodological advance in the present work is the combined use of in situ and remote sensing measurements and the outputs of the mesoscale simulations.

Study area and data set description

Kozani is a medium-size city in NW Greece, located in the south part of a mountainous basin. In the basin, four lignite combustion power stations (PS1, PS2, PS3, PS4) with stacks of 115–200 m in height are operated by the Greek Public Power Corporation with different and variable PM, NO_2 and SO_2 emissions (Triantafyllou and Kassomenos 2002; Kaldellis et al. 2012). In the north part of the basin, another electric power station is also operated (PS5). Furthermore one lignite power station (PS6) is also operating in the Former Yugoslav Republic of Macedonia (FYROM), closely to the borders of Greece and more specifically closely to the area of interest. The power stations use raw lignite as fuel that is mined nearby, through open-pit mines. The power plants lie at about 650 m above sea level. In addition to that, there are also different other types of pollution sources in this area related with urban and agricultural/burning biomass activities. Figure 1 shows the topography of the region with the power stations (PSs).

The measured data were provided from both in situ measurement station and DOAS system in the city centre. DOAS spectra were recorded using a high-pressure 150-W xenon lamp. The DOAS (SANOA, Environment S.A.) system was installed on the roofs of two opposite buildings above the busiest street in the city of Kozani. Figure 2 describes the top of the street canyon covered by the DOAS light path. The emitter and the receptor were located at a height of 10 and 15 m, respectively, above ground level covering a distance of 291 m in length. The span calibration of the DOAS system was performed by introduction of one or more gas cell with a known high concentration of the gas in interest. More details for the matter can be found in Triantafyllou et al. 2008. Concentrations of O_3, NO_2 and SO_2 have been collected from DOAS measurements. For the same period,

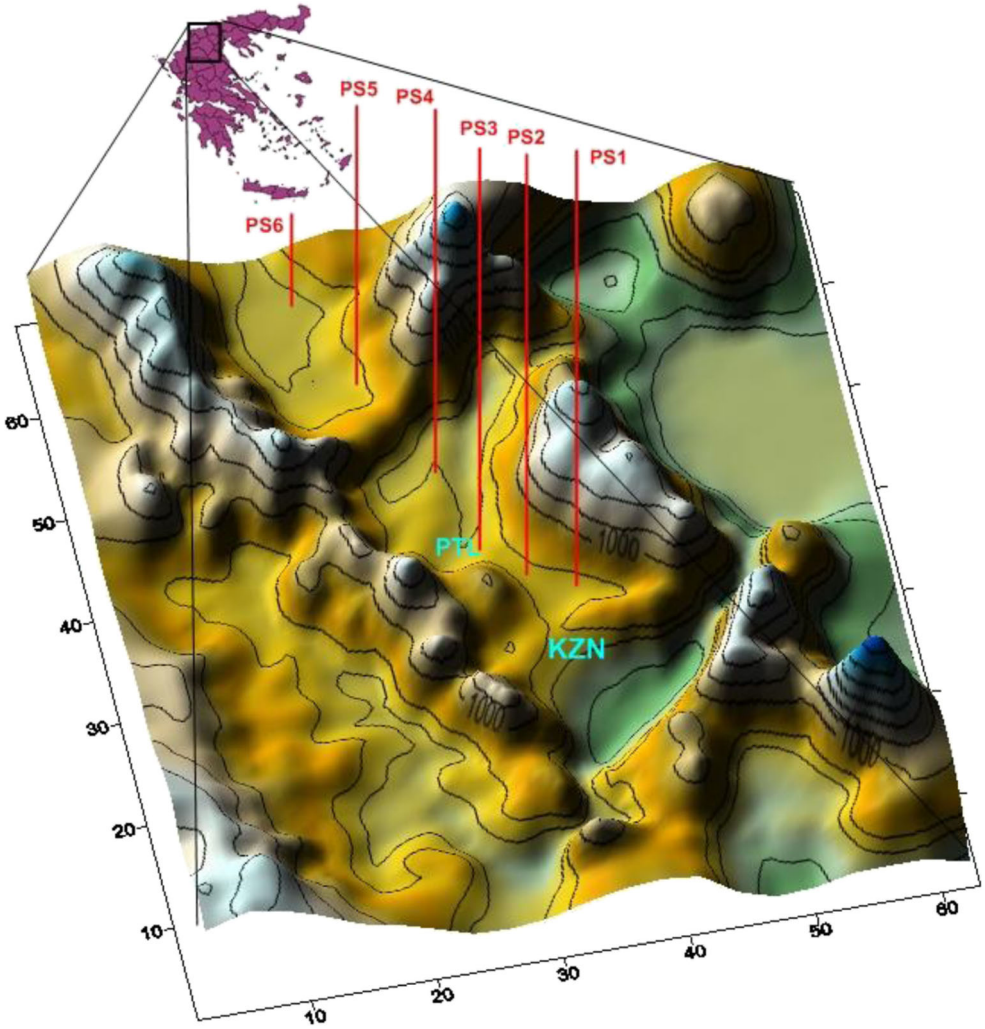

Fig. 1 Topography of the area covered by the inner grid with the power stations (PSs) (Triantafyllou et al. 2013)

experimental data of SO_2, O_3 and NO_2 from a ground measurement station located near the street canyon covered by DOAS light path have also been collected. The sampling head was operating at a height of 3 m AGL. Meteorological parameters of temperature, solar radiation, humidity, surface pressure, wind speed and direction were obtained from the meteorological station on the roof of the Technological Education Institution (TEI) of Western Macedonia, 1 km outside the city of Kozani.

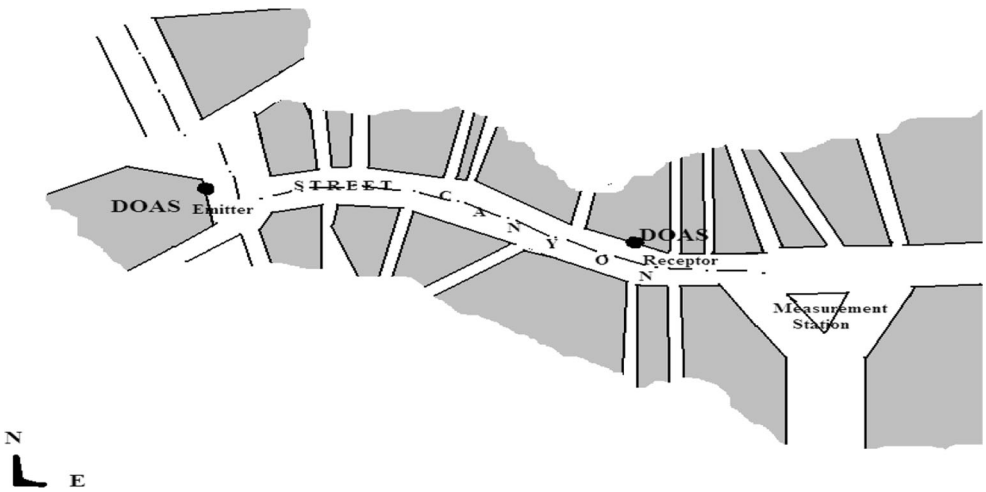

Fig. 2 Street canyon covered by DOAS light path and the measurement station location (Triantafyllou et al. 2008)

Air pollution model

Model description

The air pollution model (TAPM) is a PC-based, nestable, prognostic meteorological and air pollution model driven by a graphical user interface. TAPM solves fundamental fluid dynamics and scalar transport equations to predict meteorology and pollutant concentration for a range of pollutants important for air pollution applications. TAPM consists of coupled prognostic meteorological and air pollution concentration components, eliminating the need to have site-specific meteorological observations. Instead, the model predicts the flows important to local-scale air pollution, such as sea breezes and terrain-induced flows, against a background of larger-scale meteorology provided by synoptic analyses. For computational efficiency, it includes a nested approach for meteorology and air pollution, with the pollution grids optionally being able to be configured for a subregion and/or at finer grid spacing than the meteorological grid, which allows a user to zoom in to a local region of interest quite rapidly. The meteorological component of the model is nested within synoptic-scale analyses/forecasts that drive the model at the boundaries of the outer grid. The coupled approach taken in the model, whereby mean meteorological and turbulence fields are passed to the air pollution module every 5 min, allows pollution modelling to be done accurately during rapidly changing conditions such as in sea breeze or frontal situations. The use of integrated plume rise, Lagrangian particle, building wake and Eulerian grid modules allows industrial plumes to be modelled accurately at fine resolution for long simulations. Similarly, the use of a condensed chemistry scheme also allows nitrogen dioxide, ozone and particulates to be modelled for long periods. Details on the model approach with a more complete technical description can be found in (Hurley et al. 2003, 2005; Hurley 2005).

Model configuration

TAPM V4.0 was used in a nested mode with 25×25×25 grid points and 30, 10 and 3 km spaced horizontal grids for meteorology and with 81×81×25 grid points and 6, 2 and 0.6 km spaced horizontal grids for pollution (Fig. 3). It is worth noting that the area covered by each pollution grid is less than the area of the corresponding meteorological grid. In this way, the pollution grids avoid the boundary regions of the nested meteorological grids, where unspecified vertical velocities can sometimes occur. The lowest ten model's levels were at heights of 10, 25, 50, 100, 150, 200, 250, 300, 400 and 500 m, with the model top at 8 km.

TAPM was configured for the region of Kozani by extracting the surface information databases which are provided by CSIRO Atmospheric Research, Australia, and include gridded terrain height, vegetation and soil type, sea-surface temperature and synoptic-scale meteorology (default databases was used).

The stacks of the PSs were employed as emission sources. A chemistry mode (PM10, NO_x, NO_2, O_3, SO_2 and PM2.5) was chosen to be simulated by the model. The concept of using smog reactivity (Rsmog) rather than volatile organic compounds (VOCs) for all VOC emissions follows from the work of Johnson (1984). The concentration of Rsmog is defined as a reactivity coefficient multiplied by VOC concentration: [Rsmog]=0.0067[VOC] (Hurley 2005, TAPM Technical description, CSIRO,).

The model was run in Lagrangian mode to capture the near-source dispersion more accurately during the first 900 s and then changes to Eulerian mode, by using the TAPM option (maximum particle travel time before conversion to Eulerian grid model (EGM) (LPM)), which allows selection of the travel time after which Lagrangian particles are converted to grid concentration and from then on represented by the Eulerian transport equation (EGM mode).

Data analysis

For the validation of the results obtained by the air pollution model TAPM, the ozone concentrations from the model's first vertical level (9.3 m) were compared with the experimental data from a ground measurement station (MS). Model validation was performed also by comparing model predicted values with the recorded data of differential optical absorption spectroscopy (DOAS) that emits/receives along a street canyon in the city centre.

The statistical evaluation method proposed by Wilmott et al. (1985) is used to validate the model results and to analyse pollutants' concentration against each other and meteorology parameters, in order to reveal the most important factors in ozone production. The statistical tools were already used in other studies (e.g. Dias de Freitas et al. 2005; Papalexiou and Moussiopoulos 2006; Elbir et al. 2010). Hourly averages from monitored data were compared with hourly averages extracted from the corresponding TAPM grid cells. Three performance indices were calculated, the index of agreement (IOA), the root-mean-square-error (RMSE) and the correlation coefficient *r*.

The IOA is defined as

$$\mathrm{IOA} = 1 - \frac{\sum_{i=1}^{n} (P_i - O_i)^2}{\sum_{i=1}^{n} \left(|P_{\mathrm{i}} - O_{\mathrm{ave}}| + |O_i - O_{\mathrm{ave}}|\right)^2} \quad (1)$$

where n is the number of observations, O_{ave} is the average of the observations O_i and P_i are the simulation predictions.

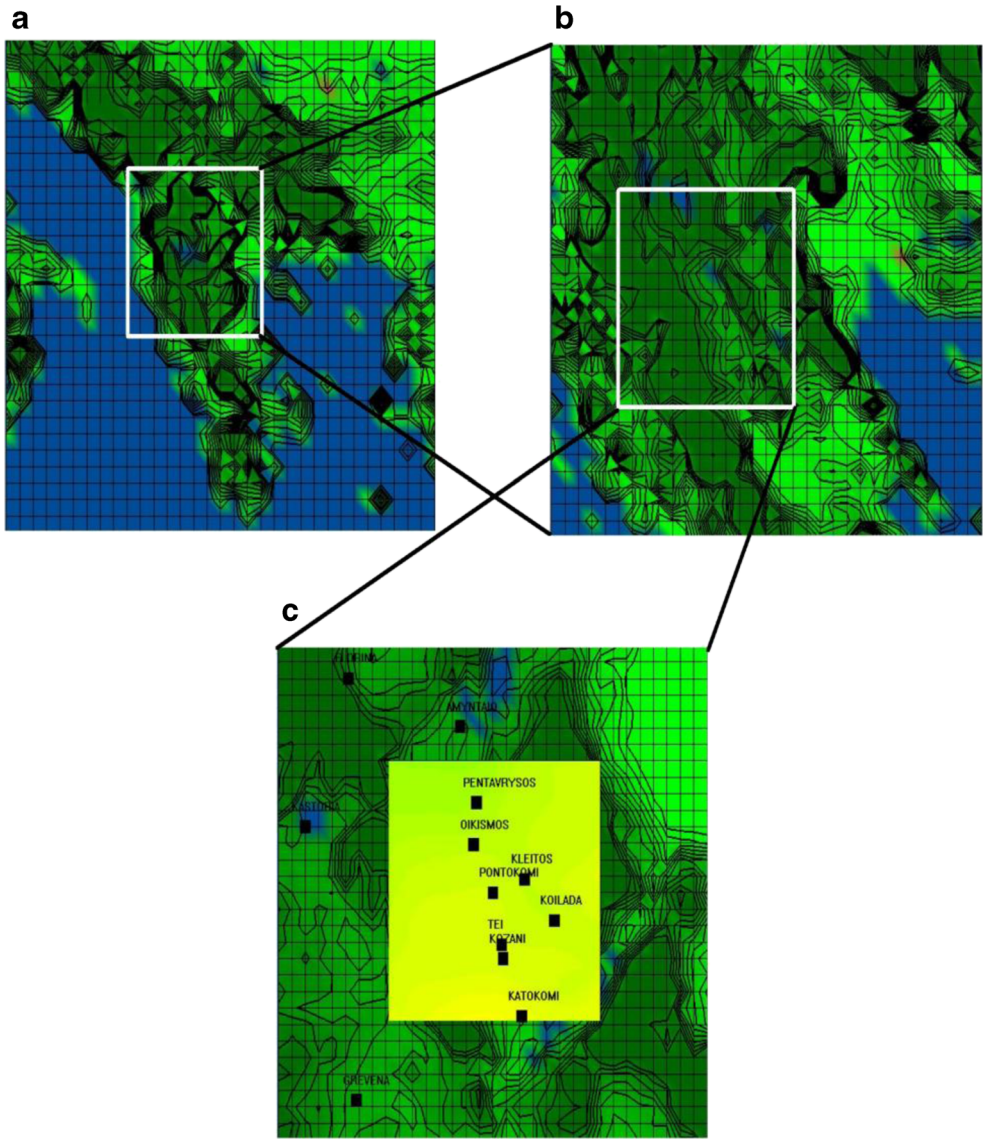

Fig. 3 TAPM grid domains, 3000 m resolution for meteorology, with west-east and south-north extent of 99 km, and 600 m resolution for pollution, extent of 48.6 km: **a** outer grid, **b** middle grid and **c** inner grid

The index of agreement ranges from 0.0, noting complete disagreement, to 1.0, indicating perfect agreement between the observed and predicted observations. The IOA is a measure of skill of the model in predicting variations about the observed mean; a value above 0.5 is considered to be good.

The error in the model was assessed using the RMSE (Eq. 2), as defined good model results assume that RMSE approaches to zero.

$$\mathrm{RMSE} = \left[\frac{1}{n}\sum_{i=1}^{n}(Oi - Pi)^2\right]^{1/2} \tag{2}$$

The correlation coefficient r (Eq. 3) is a measure of the extent to which two measurement variables "vary together". The correlation analysis tool is particularly useful when there are more than two measurement variables for each of N subjects.

$$r = \frac{N\left(\sum_{i=1}^{N} OiPi\right) - \left(\sum_{i=1}^{N} Oi\right)\left(\sum_{i=1}^{N} Pi\right)}{\sqrt{\left[N\left(\sum_{i=1}^{N} O_i^2\right) - \left(\sum_{i=1}^{N} O_i\right)^2\right]}\sqrt{\left[N\left(\sum_{i=1}^{N} P_i^2\right) - \left(\sum_{i=1}^{N} P_i\right)^2\right]}} \tag{3}$$

The correlation coefficient is a number between −1 and 1, which measures the degree to which two variables (e.g. measured and predicted values) are linearly related. Whether large values of one variable tend to be associated with large values of the other (positive correlation), whether small values of one variable tend to be associated with large values of the other

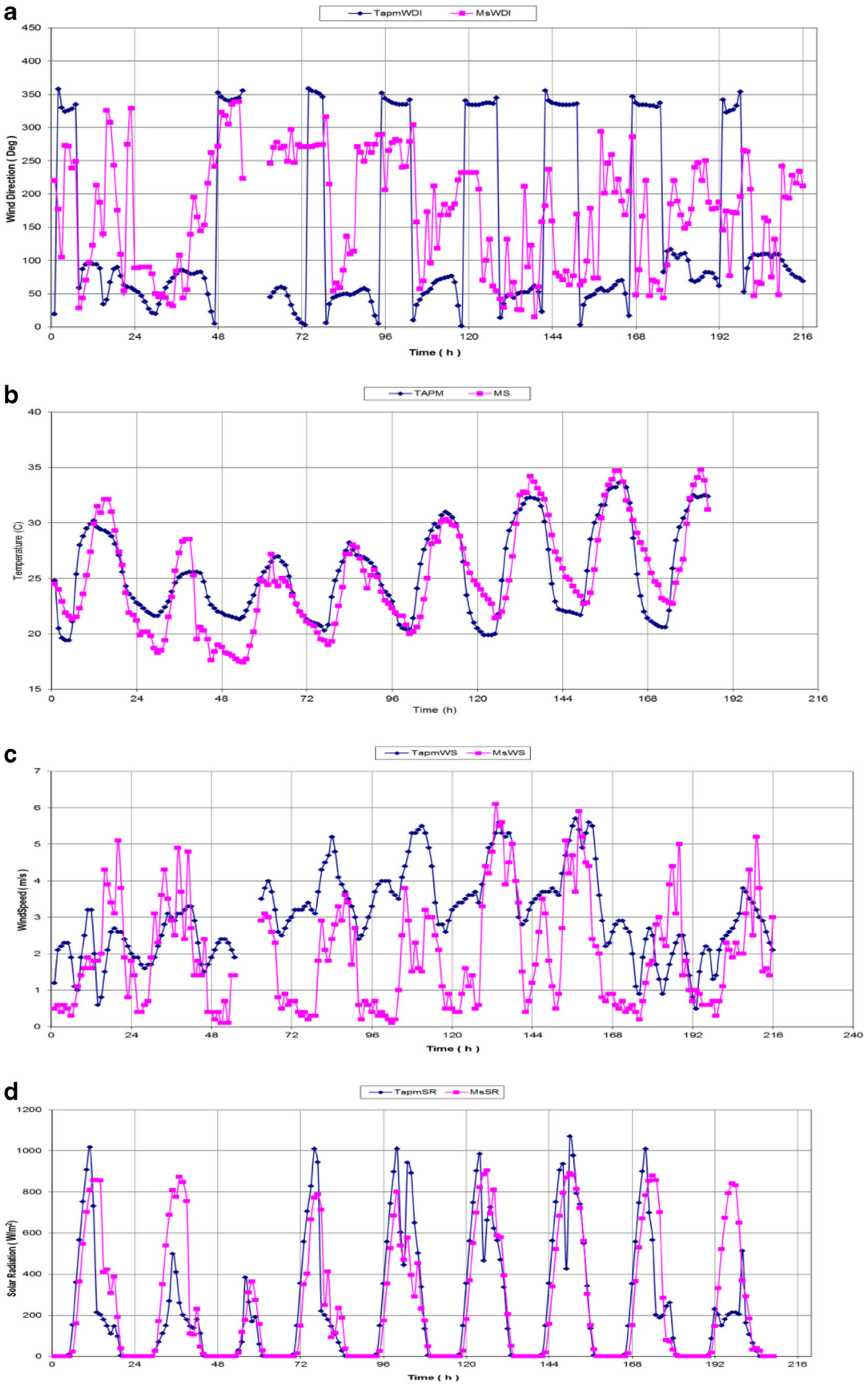

Fig. 4 Meteorological monitoring station (*MS*) compared to TAPM results for **a** wind direction, **b** temperature, **c** wind speed and **c** solar radiation (*SR*)

(negative correlation) or whether values of both variables tend to be unrelated (correlation near zero).

Simulation results and discussion

A seven-day period during June 2006 has been simulated by TAPM. This has been selected due to relatively high ozone concentrations; TAPM uses synoptic data with 1° resolution to calculate the near-surface wind field in order to further estimate pollutants' dispersion together with photochemical production.

Meteorology

The distribution of pollutants and therefore the ozone production depend on meteorological conditions such as temperature, solar radiation, wind speed and its direction. To validate the simulated meteorological fields, we compare the model results to experimentally measured parameters like temperature, solar radiation, wind speed and direction (Fig. 4a–d). They were obtained from the meteorological station on the roof of the Technological Education Institute (TEI) of Western Macedonia 1 km outside the city of Kozani. Performance statistics between TAPM meteorology results and the corresponding observed values in the meteorological station are presented in Table 1.

The first graph in Fig. 4 demonstrates that shifts in wind direction occur at the right times at the city, which means wind reversal starts and stops at the same time. The discrepancy in wind direction at the beginning and the end of each shift is mainly attributed to the proximal approximation of the grid point that nearly represents the station location and the complex topography of the area.

Temperature shows reasonable agreement for the minimum and maximum respectively at 0400 and 1500 hours, during the simulation period (Fig. 4 second graph). A slight discrepancy at minimal and maximal values may be attributed to the difficulties in accurately modelling of the lower layer and humidity content of soil (deep soil parameters).

Regarding the wind speed (Fig. 4, third graph), the difference in values is due to the location of the meteorological station and the complex topography of the area of interest. However, there is an acceptable correlation (r=0.46) between the observed and modelled values.

Table 1 Model performance statistics for meteorology

	IOA	RMSE	Correlation coefficient r
Temperature (C)	0.89	2.63	0.81
Solar radiation (W/m^2)	0.88	200.1	0.79
Wind speed (m/s)	0.62	1.88	0.46

The fourth graph gives a good comparison for the solar radiation during the period of the simulation, with a very good agreement (IOA=0.88) and a high correlation coefficient r=0.79.

Finally, we can say that the simulated meteorological fields are realistic. Temperature has shown significant agreement with the experimental data. Wind speed and direction are reproduced with wind reversal observed at the same times in the model and in measurements. Solar radiation is evaluated very well with MS data. Therefore, meteorological fields are viewed as realistic enough to drive transport and mixing of chemical species.

Figure 5 illustrates the diurnal variation of the surface level wind field calculated in the inner meteorological grid domain, at different times (0400, 0800, 1200, 1600, 2000 and 0000 hours) during 23 June 2006. As can be seen in Fig. 5, the wind circulation regime is strongly affected by the complex topography of the area. The horizontal surface wind is very weak and is formulated mainly by the local circulation patterns.

Chemistry simulation

Model's results and validation

The ozone concentrations from the model's first vertical level (9.3 m) were compared with the observations from both in situ MS and DOAS system. Figure 6 shows the observed mean hourly O_3 concentrations in Kozani city centre (MS and DOAS system) and the corresponding predicted values by the model during the simulated period (23–29, June 2006). Temporal variability of the simulated ozone concentrations corresponds reasonably well to the measured values from DOAS and MS. The higher concentrations are also observed at about the same time (1600 hours) in both, the simulation and the observations. Table 2 reports the statistical evaluation results of the ozone data obtained by the simulation against both; measurement station and DOAS data during the simulated week. The index of agreement and the correlation coefficient for TAPM simulation are 0.70 and 0.60, respectively, with the MS data; this shows a relatively high skill of TAPM to describe the situation. The corresponding values against DOAS are 0.41 and 0.63, respectively.

The difference between the concentrations of in situ measurement station, DOAS and the TAPM predictions may be because of the level and the area in which every tool took the information. So, the DOAS system's measurements represent averages over paths, while the MS gives the concentration values at a specific point which is not exactly below the DOAS path and TAPM grid point. It is also mentioned that in meteorology at the model top boundary, all variables are set at their synoptic values. This is different from the pollution

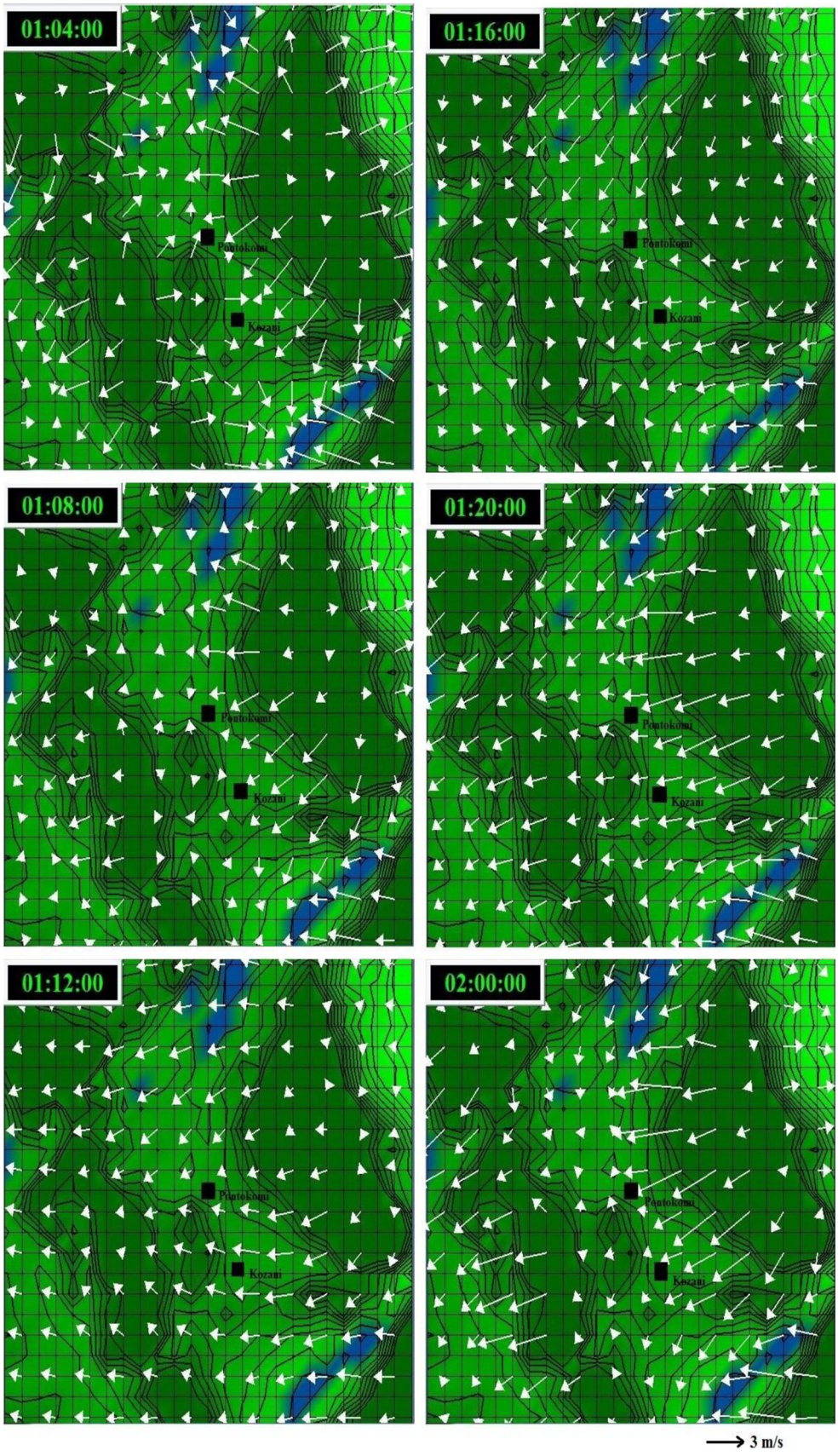

Fig. 5 Diurnal variation of the surface level wind field predicted with the model, on the inner grid domain, for the 23 June 2006. Where the time format presents: day:hour:minute

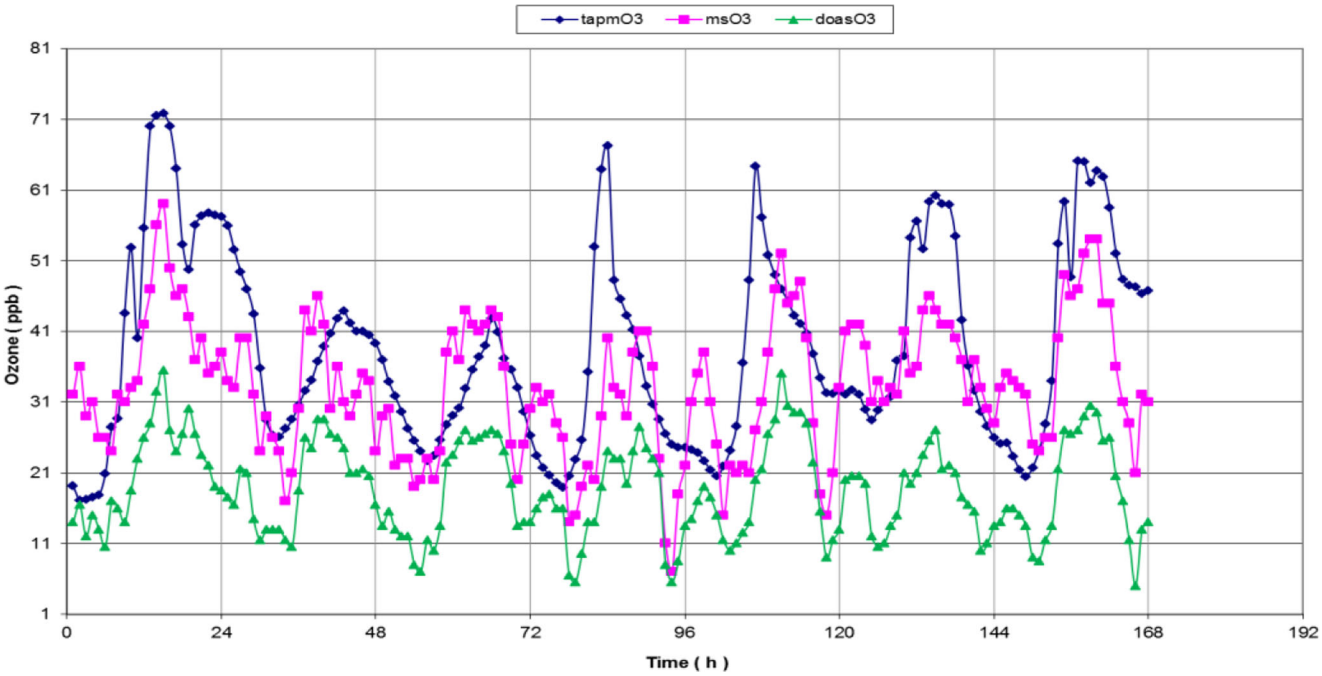

Fig. 6 Observed and predicted mean hourly ozone concentrations (ppb) in Kozani city centre, obtained by TAPM, measurement station and DOAS, during the simulated period: 23–29 June 2006

case where no boundary conditions are used, which may affect the simulation results. In addition, it is noted that during the extraction of the model results from the grid points above measurements' location (neighbouring points), the nearest grid point to the station and DOAS path was taken. It also must be taken into account that O_3 background concentrations of 20 ppb were used as input in the model, which explains the drift of the model's results.

Table 3 shows all the statistical measures of the hourly averages during the simulated period. The correlation coefficient of the hourly averages for the whole week between the observed and predicted ozone data is significantly high, 0.75 and 0.86 with MS and DOAS, respectively. Results from the model for ozone are in good agreement with the ground surface station and DOAS data. Figure 7 shows the scatter plots between the measured and predicted ozone concentrations in Kozani city for the whole period. All the DOAS data is under the line 1:1, while monitoring station (MS) data is above the line 1:1 for the small values and under it for the highest values, with slopes equal to 0.44 and 0.77 for DOAS and MS, respectively.

In NO_2 case (Fig. 8), the results obtained by TAPM are not compared well with surface data. There is also a difference between the data from the two measuring stations (DOAS and MS). This is attributed to the different traffic loads at the areas of sampling. The MS location is very close to vehicular sources emitting considerable amounts of NO_x ($NO+NO_2$). That is why its values are very high against DOAS values which are acquired from a high level (10 to 15 m) and indicate averages over the path above the street canyon. On the other hand, TAPM results represent a grid point at 10 m higher than the ground. Besides, the location of the ground sampling station is not exactly below the DOAS path and TAPM grid point.

Ozone daily variation

Figure 9 shows the ozone concentration at the first grid level (9.3 m) in the region of Kozani (inner grid), at six different times (0400, 0800, 1200, 1600, 2000 and 00:00 hours) of 23 June 2006 corresponding to daytime and nighttime, as well as the wind field. We can see the ozone formation along with the

Table 2 Model performance statistics of mean hourly ozone concentrations during the considered period

	IOA	RMSE (ppb)	Correlation coefficient *r*
Monitoring station	0.70	12.40	0.60
DOAS	0.41	22.76	0.63

Table 3 Model performance statistics of ozone's daily variation computed from the hourly averages values of the whole period

	IOA	RMSE (ppb)	Correlation coefficient *r*
Monitoring station	0.78	8.13	0.75
DOAS	0.42	20.6	0.86

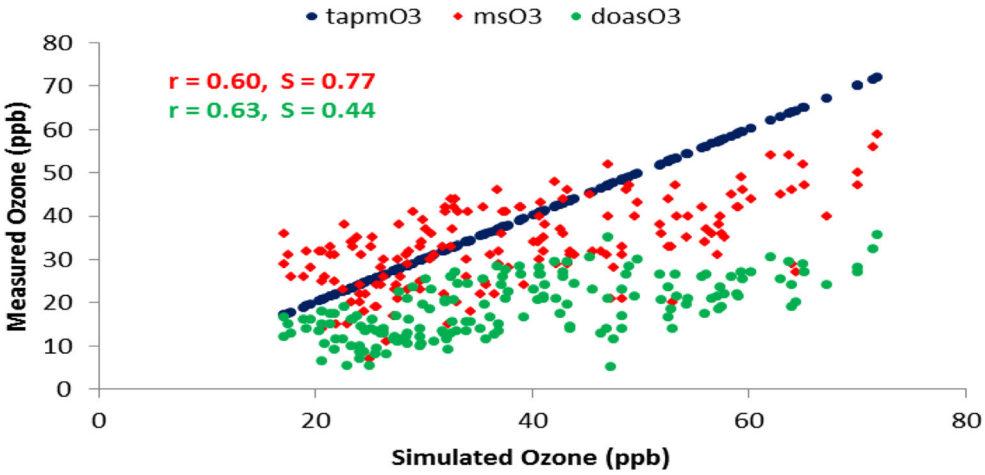

Fig. 7 Comparison between measured and simulated ozone in Kozani city centre, where r is the correlation coefficient and S is the slope

wind field and the effect of wind speed and direction on the ozone distribution during the day.

At 0400 hours, the ozone concentration is minimal. Two are the main factors that affect the ozone concentration pattern. On one hand, the inflow of ozone background and on the other hand the ozone depletion reactions due to the primary NO_x emissions. This situation is about the same until sunrise. At 0800 hours, ozone concentration starts becoming visible in the inner domain, near the power stations and the southwest of the domain. In the course of the day and until late noon, ozone formation takes place mainly above the southwest grid due to the accumulation of primary pollutants emitted from PSs and the influence of wind direction (white vectors).

Because of the photochemical operation caused by the interaction between the primary pollutants and sunlight, ozone concentration becomes a maximum at about 1600 hours. As a result of the air flow from the north and east, high ozone concentration levels moved to the southeast part of the domain. In the evening, the ozone concentration decreased at 2000 hours, and after midnight, the early morning situation is re-established. In all the period of simulation, almost the same scheme was repeated with difference in

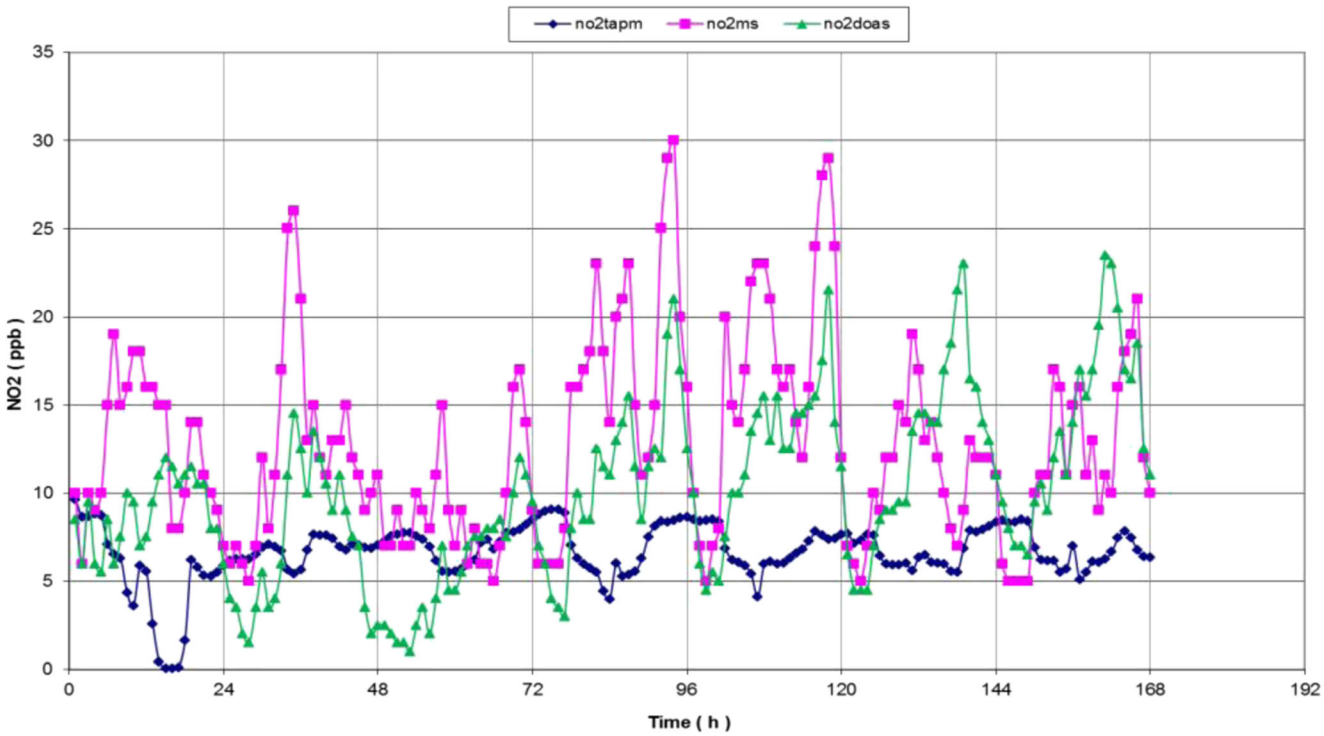

Fig. 8 Concentrations of NO_2 in Kozani city centre, obtained by TAPM, measurement station and DOAS, during the simulated period between 23 and 29 June 2006

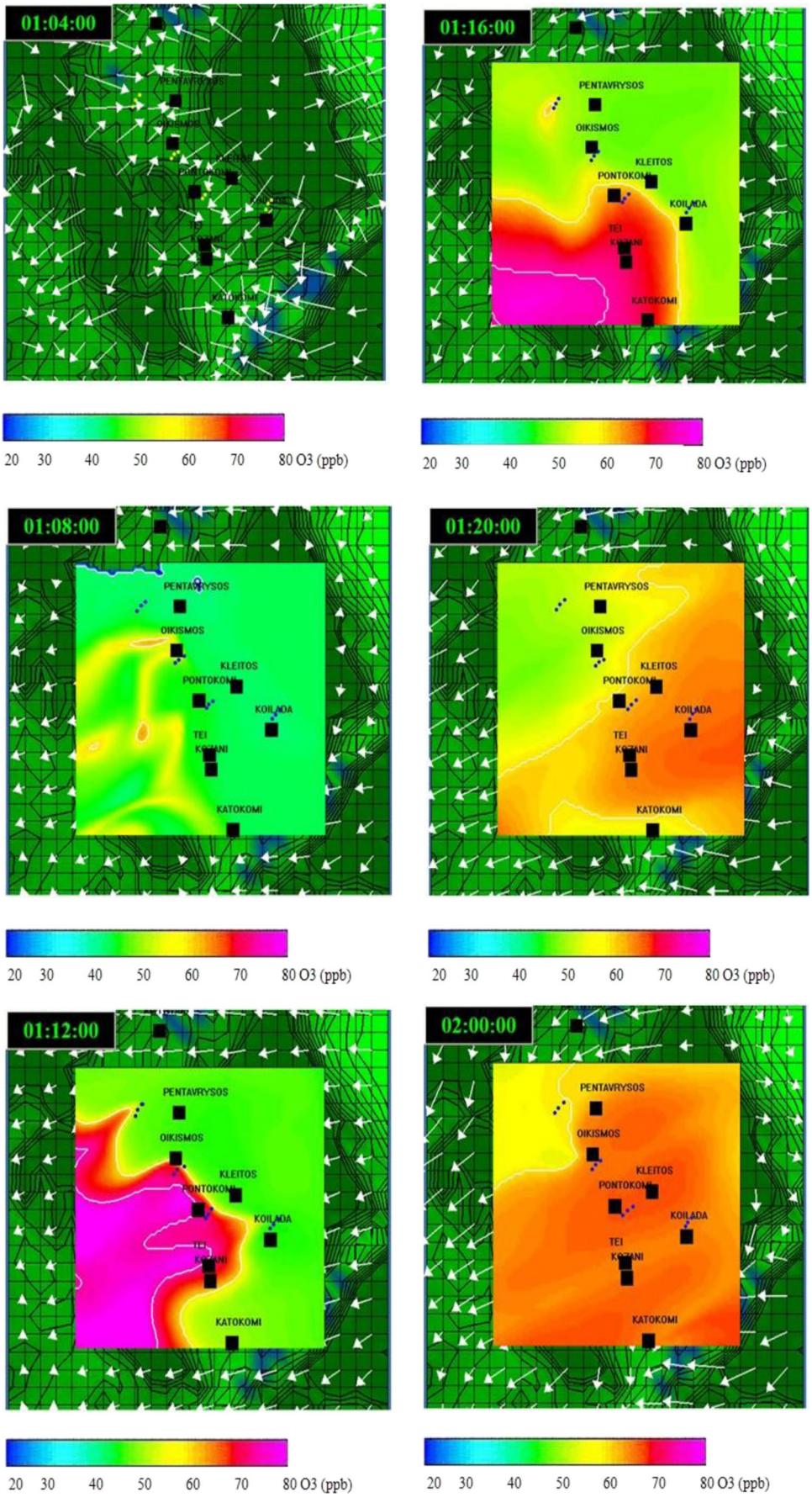

Fig. 9 Diurnal variation of the surface level ozone concentration field and wind field (*white vectors*) predicted by TAPM, for 23 June 2006. Where the time format presents: day:hour:minute

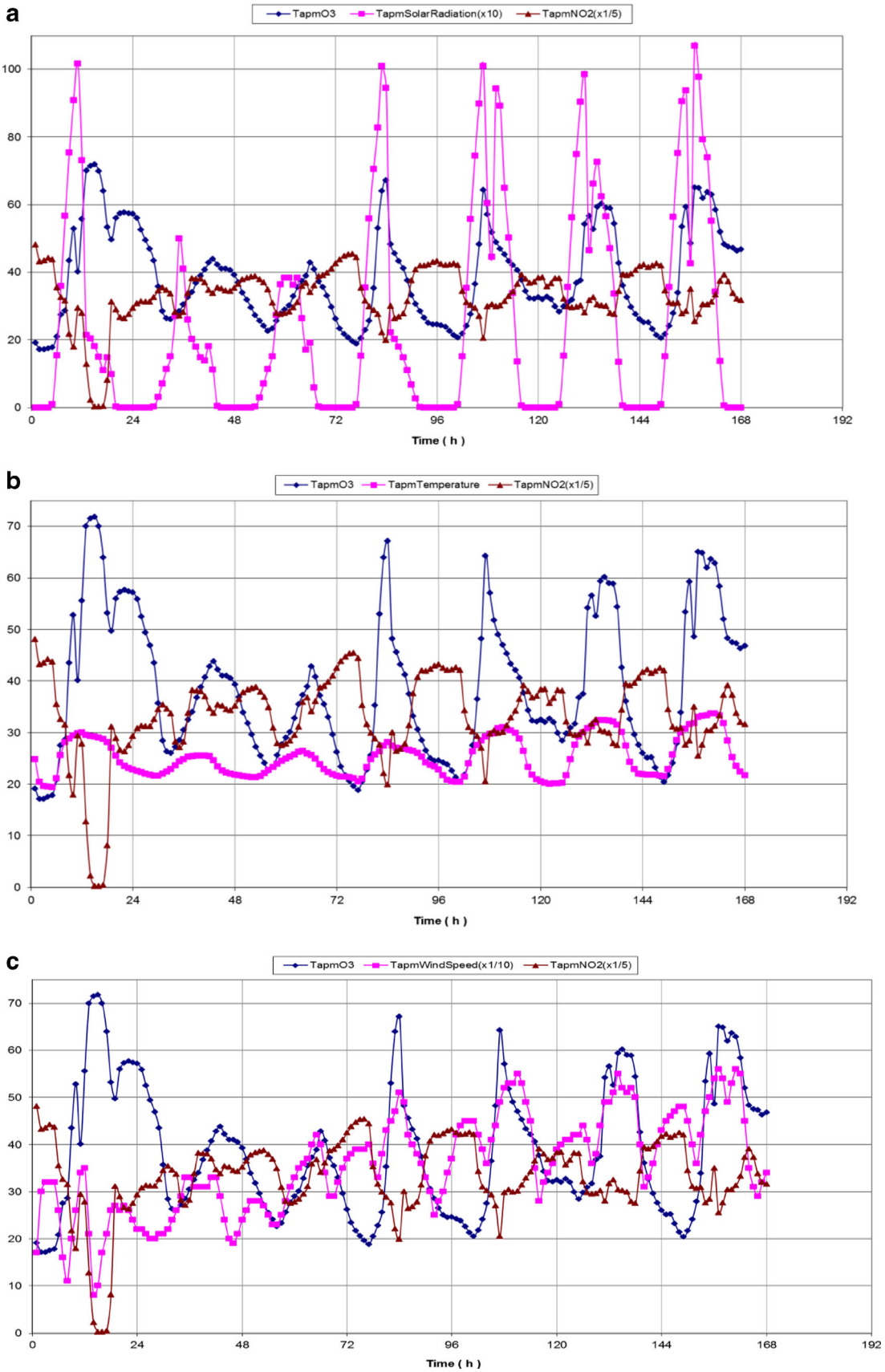

Fig. 10 The variation of ozone and NO_2 concentrations in Kozani city centre with solar radiation (**a**), temperature (**b**) and wind speed (**c**), during the simulated period

the concentration's level. The maximum level of daily ozone concentration in Kozani city is observed at 1600 hours, as it is also shown in Fig. 9.

In order to investigate the stacks' emissions' effects and contribution regarding the O_3 concentrations in the city of Kozani, two simulations were carried out, the one with and the other without PSs emissions' sources (in the second case, only background concentrations of pollutants were used). The comparison between the two cases proved that the contribution of the emissions from the PSs to O_3 pollution in the city of Kozani is strongly influenced from the background concentrations, which were used as input in the model. This reveals the importance of reliable background concentrations of pollutants for efficient prediction. In any case, the problem of the high stacks' emissions' contribution to the O_3 formation in adjacent complex terrain urban area is under further investigation in the Laboratory of Atmospheric Pollution and Environmental Physics (LAP-EP).

Figure 10a–c and Table 4 show the effect of the meteorology conditions (temperature, solar radiation and wind speed) on the formation of ozone and NO_2 during the simulated period.

Figure 10a, b displays that high ozone concentrations coincide with high temperature and solar radiation and low NO_2 concentrations, which explains the photochemical operation between primary pollutants and sunlight, resulting in ozone production. This symmetric level has occurred between ozone and NO_2 which follow opposite trends with a correlation coefficient of −0.70. It is worthwhile to be mentioned here that Triantafyllou et al. 2008 have found the correlation coefficient between O_3 and NO_2 is equal to −0.59 by using one year's concentration measurements of the MS.

A steady rise in the ozone level is observed with decreased NO_2 concentration. The peak concentration of NO_2 occurs before the peak of ozone, because the photochemical reaction sequence forms NO_2 first and then ozone. The above hints show the favourable photochemical ozone production within the urban complexity between the morning hours and up to the afternoon.

Figure 10c illustrates the relation between O_3, NO_2 and wind speed. As shown in this graph, when the horizontal wind speed increases, ozone concentration increases too, as fresh oxygen is supplied in the photochemical cycle reacting with NO_2 and finally leading to the production of O_3. In addition, wind contributes to the dilution of the atmospheric mass bringing these more photochemically reactive molecules under the sunlight's influence (Triantafyllou et al. 2008).

Table 4 presents the correlation coefficient between ozone, NO_2, temperature and solar radiation. A good correlation between ozone and meteorology was found; specifically, the correlation coefficient found is equal to 0.71 and 0.46 for temperature and solar radiation, respectively. Negative correlation between NO_2 and meteorology parameters, with −0.53 against temperature and −0.46 against solar radiation, was found. These findings confirm the factors that drive the photochemical phenomena.

Table 4 The correlation coefficient r of chemical and meteorological TAPM results

Correlation coefficient r	Ozone	NO_2
Temperature	0.71	−0.53
Solar radiation	0.46	−0.46
Wind speed	0.29	0.004
NO_2	−0.70	1

Summary and conclusions

The objective of this work was to investigate the photochemical smog formation, the dispersion and concentration of O_3 and NO_2, as well as the meteorology effects, over a heavily industrialized area in Greece. The region is a mountainous basin with complex terrain, which results in the local meteorological circulations observed. A coupled mesoscale prognostic meteorological and air pollution model in combination with data, which were collected by in situ and remote monitoring measurements, was used. More specific, three-dimensional photochemical simulations have been performed by The Air Pollution Model (TAPM) for a seven-day period in the summer of 2006. A model configuration including the industrial sources has been built to simulate the pollutants' dispersion and transformation in and around Kozani, the most populated city of the area. Results from the numerical simulation were compared with the observations of both in situ monitoring station and DOAS, which have been installed in the city centre. Comparison of model's results to observations at the city centre showed the considerable skill of the model (TAPM) in predicting the major mesoscale features affecting the pollutants' dispersion and concentrations in the area of interest.

Simulated meteorological fields were viewed as realistic enough to drive transport and the mixing of chemical species. More specifically, temperature has shown significant agreement against experimental data. Wind speed and direction were reproduced with wind reversal observed at the same times in the model as in the measurements. Solar radiations were evaluated very well against monitoring station data.

Regarding the O_3 concentrations, the statistical performance measures (IOA, RMSE and correlation coefficient) indicated a good agreement between the predicted and observed O_3 values. However, there were some differences between predicted and measured values maybe due to the level where each tool (TAPM, DOAS and MS) captured the information, while the drift of the simulation's results is due to relatively high

background concentrations which were used as input in the model. In any case, in the LAP-EP, this evaluation is an ongoing activity.

Concerning the NO_2, the simulated values were not compared well with surface data. Differences were also observed between the data sets collected by DOAS system and MS. The MS location is very close to vehicular sources emitting considerable amounts of NO_x. That is why its values are higher than DOAS values which are acquired from a high level (10 to 15 m) and indicate averages over the path above the street canyon. On the other hand, TAPM results represent a grid point at 10 m higher than the ground. Besides, the location of the ground sampling station is not exactly below the DOAS path and TAPM grid point.

A comparison between pollutants (O_3, NO_2) and meteorology parameters (temperature, solar radiation and wind speed) has shown clearly the photochemical process where the primary pollutants and sunlight react to produce ozone. The statistical analyses showed a negative agreement between NO_2 against temperature and solar radiation. On the other hand, a good agreement has been achieved between temperature, solar radiation and ozone. TAPM simulation and experimental data have shown that as wind speed increases, the concentration of ozone increases because fresh oxygen is supplied in the photochemical cycle that reacts with NO_2 producing O_3. This highlights clearly the effects of meteorology conditions and topography on the air pollution smog formation.

In addition, a very interesting symmetric level has occurred between ozone and NO_2 which follow opposite trends. A steady rise in the ozone level is observed with decreased NO_2 concentration. The peak concentration of NO_2 occurs before the peak of ozone because the photochemical reaction sequence forms NO_2 first and then ozone. This shows the favourable photochemical ozone production within the urban complexity between the morning hours and 1800 hours in the afternoon.

The ozone levels in the city of Kozani are kept at a relatively high levels' concentration even without being close to the industrial sources because of the wind regime effects.

Simulations have shown that the importance of reliable background concentrations of pollutants in the area of interest is related to experimental data to predict efficiently even without an overall emission inventory. Numerical simulation data of photochemical pollutants were significantly correlated against meteorology during the simulated period. The obtained results have contributed to the verification of distant pollutants' transfer from industrial sources.

Acknowledgments Financial support was supported by the MADEPODIM programme in frame of TEMPUS III, and computations are done in the Laboratory of Atmospheric Pollution and Environmental Physics (LAP-EP), Technological Education Institute (TEI) of Western Macedonia, Kila, 501 00 Kozani, Greece.

References

Allen C, Durrenberger C (2002) Acceleration science evaluation of ozone formation in the Houston-Galveston area. University of Texas

Bernard SM, Samet JM, Grambsch A, Ebi KL, Romieu I (2001) The potential impacts of climate variability and change on air pollution-related health effects in the United States. Environ Health Perspect 109:199–209

Brulfert G, Chemel C, Chaxel E, Chollet JP (2005) Modelling photochemistry in alpine valleys. Atmos Chem Phys 5:2341–2355

Brunelli U, Piazza V, Pignato L, Sorbello F, Vitabile S (2007) Two-days ahead prediction of daily maximum concentrations of SO2, O3, PM10, NO2, CO in the urban area of Palermo, Italy. Atmos Environ 41:2967–2995

Chen KS, Ho YT, Lai CH, Chou YM (2003) Photochemical modeling and analysis of meteorological parameters during ozone episodes in Kaohsiung, Taiwan. Atmos Environ 37:1811–1823

Couach O, Balin I, Jiménez R, Ristori P, Perego S, Kirchner F, Simeonov V, Calpini B, van den Bergh H (2003) An investigation of ozone and planetary boundary layer dynamics over the complex topography of Grenoble combining measurements and modeling. Atmos Chem Phys 3:549–562

Di Sabatino S, Buccolieri R, Pulvirenti B, Britter R (2007) Simulations of pollutant dispersion within idealised urban-type geometries with CFD and integral models. Atmos Environ 41:8316–8329

Dias de Freitas E, Droprinchinski Martins L, da Silva Dias PL, Fatima de Andrade M (2005) A simple photochemical module implemented in RAMS for tropospheric ozone concentration forecast in the metropolitan area of Sao Paulo, Brazil: coupling and validation. Atmos Environ 39:6352–6361

Elbir T, Kara M, Bayram A, Altiok H, Dumanoglu Y (2010) Comparison of predicted and observed PM10 concentrations in several urban street canyons. Air Qual Atmos Health 4:121–131

Gilliliand AB, Hogrefe C, Pinder RW, Godowitch JM, Foley KL, Rao ST (2008) Dynamic evaluation of regional air quality models: assessing changes in O3 stemming for changes in emissions and meteorology. Atmos Environ 42(20):5110–5123

Godowitch JM, Gilliam RC, Rao ST (2011) Diagnostic evaluation of ozone production and horizontal transport in a regional photochemical air quality modeling system. Atmos Environ 45: 3977–3987

Hurley P (2005) The air pollution model (TAPM) version 3. Part 1: technical description, CSIRO atmospheric research technical paper no. 71. Available at http://www.dar.csiro.au/TAPM

Hurley P, Manins P, Lee S, Boyle R, Ng Y, Dewundege P (2003) Year-long, high-resolution, urban airshed modelling: verification of TAPM predictions of smog and particles in Melbourne. Australia Atmos Environ 37:1899–1910

Hurley P, Physick WL, Luhar AK (2005) TAPM: a practical approach to prognostic meteorological and air pollution modelling. Environ Model Software 20:737–752

Johnson GM (1984) A simple model for predicting the ozone concentration of ambient air. Proceedings of the 8th International Clean Air and Environment Conference, New Zealand, Clean Air Society of Australia & New Zealand

Kaldellis JK, Kapsali M, Emmanouilidis M (2012) Long-term evaluation of nitrogen oxides and sulphur dioxide emissions from the Greek lignite-based electricity generation sector. Fresenius Environ Bull 21(9):F-2012–F-2197

Ling ZH, Guo H, Cheng HR, Yu YF (2011) Sources of ambient volatile organic compounds and their contributions to photochemical ozone formation at a site in the Pearl River Delta, southern China. Environ Pollut 159:2310–2319

Linkov I, Loney D, Cormier S, Satterstrom FK, Bridges T (2009) Weight-of-evidence evaluation in environmental assessment: review of

qualitative and quantitative approaches. Sci Total Environ 407: 5199–5205

Moussiopoulos N, Papalexiou S, Sahm P (2006) Wind flow and photochemical air pollution in Thessaloniki, Greece. Part I: simulations with the European zooming model. Environ Model Softw 21:1741–1751

Nam J, Kimura Y, Vizuete W, Murphy C, Allen DT (2006) Modeling the impacts of emission events on ozone formation in Houston, Texas. Atmos Environ 40:5329–5341

Napelenok SL, Foley KM, Kang D, Mathur R, Pierce T, Rao ST (2011) Dynamic evaluation of regional air quality model's response to emission reductions in the presence of uncertain emission inventories. Atmos Environ 45:4091–4098

Palaciosa M, Kirchner F, Martilli A, Clappier A, Martin F, Rodriguez ME (2002) Summer ozone episodes in the Greater Madrid area. Analyzing the ozone response to abatement strategies by modelling. Atmos Environ 36:5323–5333

Papalexiou S, Moussiopoulos N (2006) Wind flow and photochemical air pollution in Thessaloniki, Greece. Part II: statistical evaluation of European zooming model's simulation results. Environ Model Softw 21:1752–1758

Peng Y-P, Chen K-S, Wang H-K, Lai C-H, Lin M-H, Lee C-H (2011) Applying model simulation and photochemical indicators to evaluate ozone sensitivity in southern Taiwan. J Environ Sci 23:790–797

Pontiggia M, Derudi M, Busini V, Rota R (2009) Hazardous gas dispersion: a CFD model accounting for atmospheric stability classes. J Hazard Mater 171:739–747

Triantafyllou AG (2001) PM10 pollution episodes as a function of synoptic climatology in a mountainous industrial area. Environ Pollut 112(3):491–500

Triantafyllou AG, Kassomenos PA (2002) Aspects of atmospheric flow and dispersion of air pollutants in a mountainous basin. Sci Total Environ 297:85–103

Triantafyllou AG, Helmis CG, Asimakopoulos DN, Soilemes AT (1995) Boundary layer evolution over large and broad mountain basin. Theor Appl Climatol 52:19–25

Triantafyllou AG, Kiros E, Evagelopoulos V (2002) Respirable particulate matter at an urban and nearby industrial location: concentrations and variability and synoptic weather conditions during high pollution episodes. J Air Waste Manage Assoc 52:174–185

Triantafyllou AG, Zoras S, Evagelopoulos V, Garas S, Diamantopoylos C (2008) DOAS measurements above an urban street canyon in a medium sized city. Glob NEST 10:160–167

Triantafyllou AG, Krestou A, Matthaios V (2013) Source-receptor relationships by using dispersion model in a lignite burning area in western Macedonia, Greece. Glob NEST J 15(2):195–203

Vlachokostas C, Achillas C, Moussiopoulos N, Kalogeropoulos K, Sigalas G, Kalognomou E, Banias G (2010a) Health effects and social costs of particulate and photochemical urban air pollution: a case study for Thessaloniki, Greece. Air Qual Atmos Health. doi:10.1007/s11869-010-0096-1

Vlachokostas C, Nastis S, Achillas C, Kalogeropoulos K, Karmiris I, Moussiopoulos N, Chourdakis E, Banias G, Limperi N (2010b) Economic damages of ozone air pollution to crops using combined air quality and GIS modelling. Atmos Environ 44:3352–3361

Wang X, Carmichael G, Chen D, Tang Y, Wang T (2005) Impacts of different emission sources on air quality during March 2001 in the Pearl River Delta (PRD) region. Atmos Environ 39:5227–5241

Wilmott CJ, Ackleson SG, Davis RE, Feddema JJ, Klink KM, Legates DR, O'Donnell J, Rowe CM (1985) Statistics for the evaluation and comparison of models. J Geophys Res 90:8995–9005

Zhou W, Cohan DS, Napelenok SL (2013) Reconciling NOx emissions reductions and ozone trends in the U.S., 2002–2006. Atmos Environ 70:236–244